LAWRENCE
LIVERMORE
NATIONAL
LABORATORY

LLNL-JRNL-403927

Lithospheric Thickness Modeled from Long Period Surface Wave Dispersion

M. E. Pasyanos

May 15, 2008

Tectonophysics

Disclaimer

Lithospheric thickness modeled from long period surface wave dispersion

Michael E. Pasyanos

Lawrence Livermore National Laboratory
Livermore CA 94551 USA
Tel: (925) 423-6835
FAX: (925) 423-4077
email: pasyanos1@llnl.gov

Abstract

The behavior of surface waves at long periods is indicative of subcrustal velocity structure. Using recently published dispersion models, we invert surface wave group velocities for lithospheric structure, including lithospheric thickness, over much of the Eastern Hemisphere, encompassing Eurasia, Africa, and the Indian Ocean. Thicker lithosphere under Precambrian shields and platforms are clearly observed, not only under the large cratons (West Africa, Congo, Baltic, Russia, Siberia, India), but also under smaller blocks like the Tarim Basin and Yangtze craton. In contrast, it is found that remobilized Precambrian structures like the Saharan Shield and Sino-Korean Paraplatform do not have well-established lithospheric keels. The thinnest lithospheric thickness is found under oceanic and continental rifts, as well as along convergence zones. We compare our results to thermal models of continental lithosphere, lithospheric cooling models of oceanic lithosphere, lithosphere-asthenosphere boundary (LAB) estimates from S-wave receiver functions, and velocity variations of global tomography models. In addition to comparing results for the broad region, we examine in detail the regions of Central Africa, Siberia, and Tibet. While there are clear differences in the various estimates, overall the results are generally consistent. Inconsistencies between the estimates may be due to a variety of reasons including lateral and depth resolution differences and the comparison of what may be different lithospheric features.

Keywords: lithosphere, lithospheric thickness, upper mantle, surface waves, Eurasia, Africa

1. Introduction and Motivation

The lithosphere-asthenosphere boundary (LAB) is a rheological and mechanical boundary between the rigid lithosphere and the more freely-flowing asthenosphere. As such, seismic methods are not always thought of as the best way to derive information about this boundary and rather are often studied with thermal and rheological information. Lithospheric thickness, however, both affects and is affected by important fundamental seismological observations, such as surface wave dispersion and travel time. For instance, lithospheric thickness determines whether regionally-propagating Pn and Sn waves beyond near-regional distances travel as deeper-diving upper mantle waves (in thick lithosphere regions), or more like true head waves (in regions with thin lithosphere). This has a large bearing on the travel times of these phases.

The sensitivity kernels of long period surface waves (**Fig. 1a**) sample the subcrustal lithosphere and asthenosphere, allowing us to model lithospheric structure. For example, in **Fig. 1b**, given the same crustal structure, the dispersion at long periods changes dramatically depending on the thickness of the lid. In particular, there is a large difference in the velocity and gradient of the dispersion curve at periods of around 100 sec.

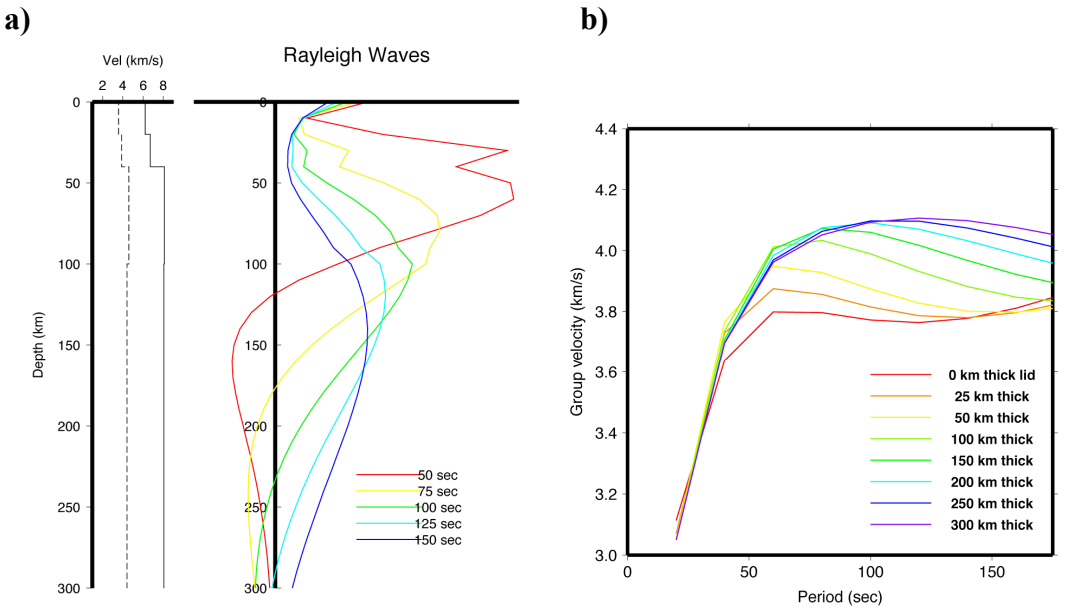

Fig. 1. a) Velocity profile and associated sensitivity kernels for long period Rayleigh waves; b) Dispersion for a model where the thickness of the lid is varied from 0 – 300 km.

The distinction is easily seen in the seismic data. For example, in **Fig. 2**, we show some contrasting examples of dispersion curves from two regions. The first, from Eastern Europe, show fast long-period group velocities that increase with period, which is indicative of thick lithosphere. The second example, from Western Europe, shows slower long-period group velocities that decrease with period at the long-period end. This is indicative of thinner lithosphere that samples the asthenosphere at shorter periods than the other example.

It is natural to ask, then, how do the seismic (surface wave) estimates of lithospheric thickness compare to other seismic and non-seismic estimates of this parameter? For example, as discussed in Jaupert et al. (1998) and Jaupert and Marescal (1999), what is described as the thermal lithosphere might not be the same as the seismic boundary. Still, it is clear that seismic waves, particularly surface waves, bring a lot of information to the problem because of their excellent coverage of the globe, in both seismic and aseismic areas, as well as in both oceanic and continental regions.

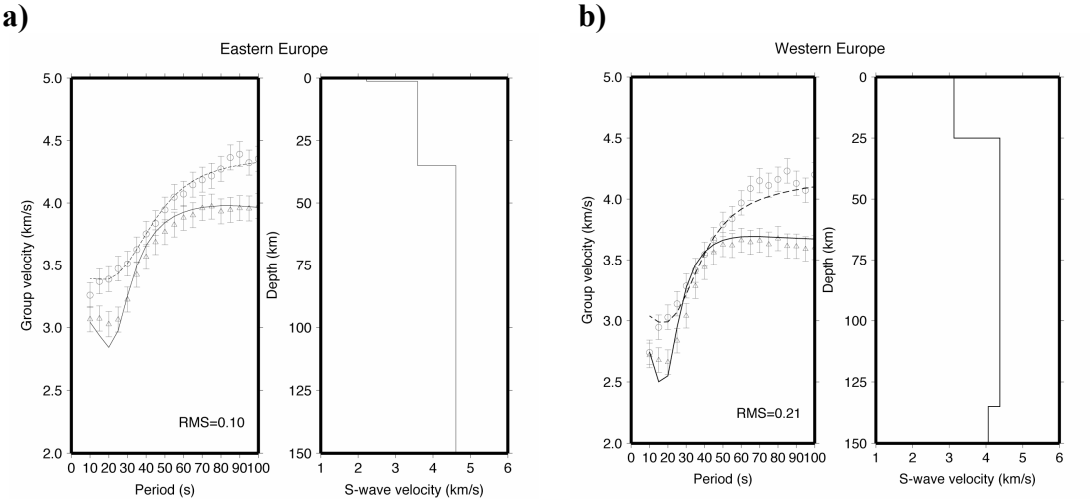

Fig. 2. a) Rayleigh wave (triangles) and Love wave (circles) measurements and model fits (solid and dashed lines, respectively) of dispersion (left) and S-wave velocity profile (right) from Eastern Europe. b) Same plots for Western Europe.

Several previous efforts have been made at providing large-scale maps of lithospheric thickness. Using heat flow data, Artemieva and Mooney (2001) constructed a global map of lithospheric thermal thickness, which was subsequently updated with the TC1 model (Artemieva, 2006). Conrad and Lithgow-Bertelloni (2006) constructed an estimated lithospheric thickness model in order to provide a depth-dependent viscosity model that varies laterally. The model was not inverted for in the traditional sense, but rather inferred from the characteristic thickness for oceanic lithosphere of a given age and derived from a tomographic model under the continents. The model is also too smooth to provide detailed tectonic insight. Here, we would like to develop a high-resolution lithospheric thickness model developed solely from long-period surface-wave dispersion data.

In this paper, we will first discuss the surface wave data and models, along with the methodology used to estimate lithospheric structure from surface waves. Next, we will report on our results for lithospheric thickness, and discuss how the results compare to tectonic features. We will then review several other lithospheric thickness estimates from heat flow, thermal cooling, 3-D seismic tomography models, and S-wave receiver functions. Lastly, we will systematically compare these other results to our own, both in a broad sense, and then in detail in a few particular regions.

2. Data and Methodology

We are utilizing the surface wave dispersion data of Pasyanos (2005) in this study (**Fig. 3**). The model consists of about 41,000 quality Rayleigh wave group velocity paths and 30,000 quality Love wave group velocity paths. As shown in **Fig. 3a**, this provides coverage of Eurasia, Africa, Indian Ocean, Arctic Ocean, and parts of the Pacific and Atlantic Oceans. From this model, we perform tomographic inversions at a number of periods, such as the 80 sec Rayleigh wave model shown in **Fig. 3b**.

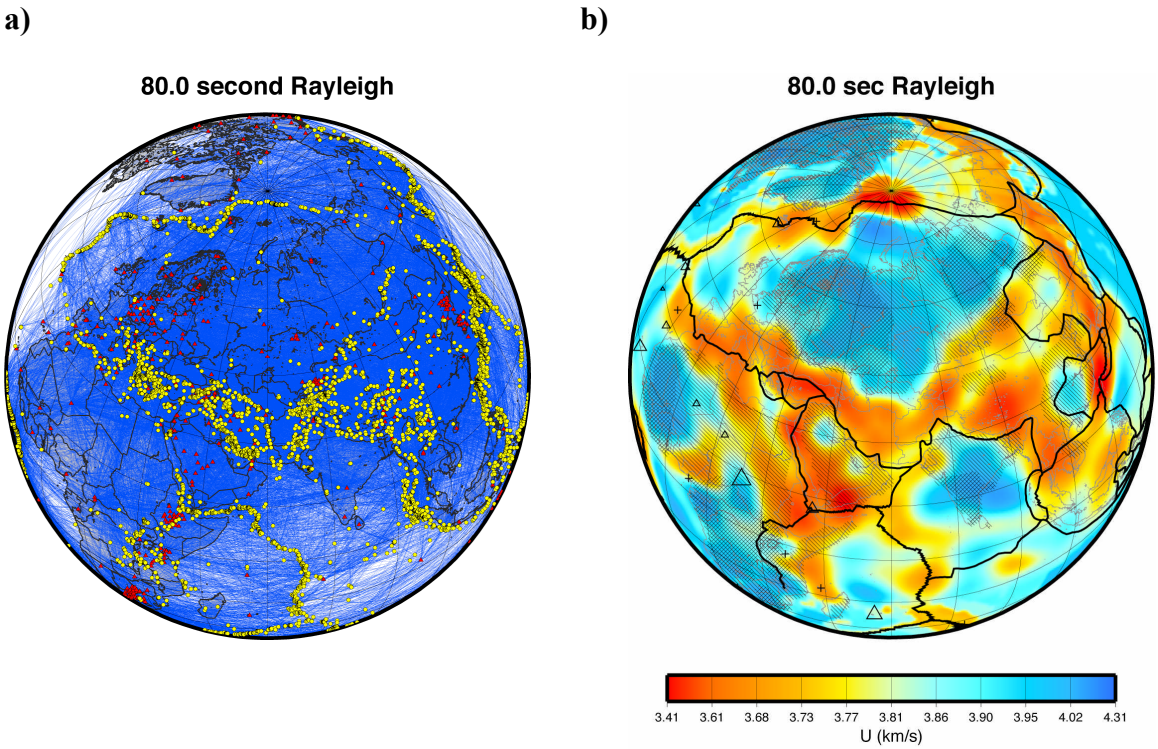

Fig. 3. a) Map of surface wave dispersion paths (blue lines) for 80 sec Rayleigh waves with events (yellow circles) and stations (red triangles) indicated. b) Map of surface wave group velocity (in km/s) for 80 sec Rayleigh waves.

The surface wave models range from 5 to 200 seconds period, although the models are probably only well-resolved everywhere between 7 to 120 seconds. Because of the dense path coverage, the resolution of the model is fairly high, but fundamentally limited at long periods by the long wavelengths. For example, the wavelength of a 100 sec surface wave is about 400 km and can realistically have a best resolution on the order of the half-wavelength or 200 km.

There have been several methods proposed to estimate the thickness of the lithosphere using seismic models. For example, Weeraratne et al. (2003) used the depth of the maximum velocity gradient (negative gradient) to define the base of the lithosphere. Here, we take a slightly different approach. We used a restricted model where a well-specified asthenosphere that underlies the lithosphere is built (hard-wired) into the model (**Fig. 4**). The LAB is simply the interface between these two defined layers.

We use a grid search to derive layered velocity structure from the surface wave group velocities. We basically use the same method as that used in Pasyanos and Nyblade (2007), with a modification to specify slabs at depth. First, we fix the sediments to that from the Laske sediment profile (Laske and Masters, 1997) shown as item 1 in **Fig. 4**. We then solve for $\overline{v}_p$ and $\overline{v}_s$ (the average P-wave and S-wave velocities of the one-layer crystalline crust) indicated as item 2, crustal thickness (item 3), Pn and Sn velocity (the P-wave and S-wave velocities of the uppermost mantle or lid) indicated as item 4, and lithospheric thickness (item 5). The v_p/v_s ratio in the crust and upper mantle lid is fixed

using a Poisson's ratio of σ=0.26. The asthenosphere (item 6) is specified to have a lower v_p and higher Poisson's ratio (σ=0.29) than the overlying lithosphere, making the shear-wave velocity in this layer (which the surface waves are primarily sensitive to) very low. The remainder of the upper mantle (item 7) is transitioned into the ak135 model (Kennett et al., 1995).

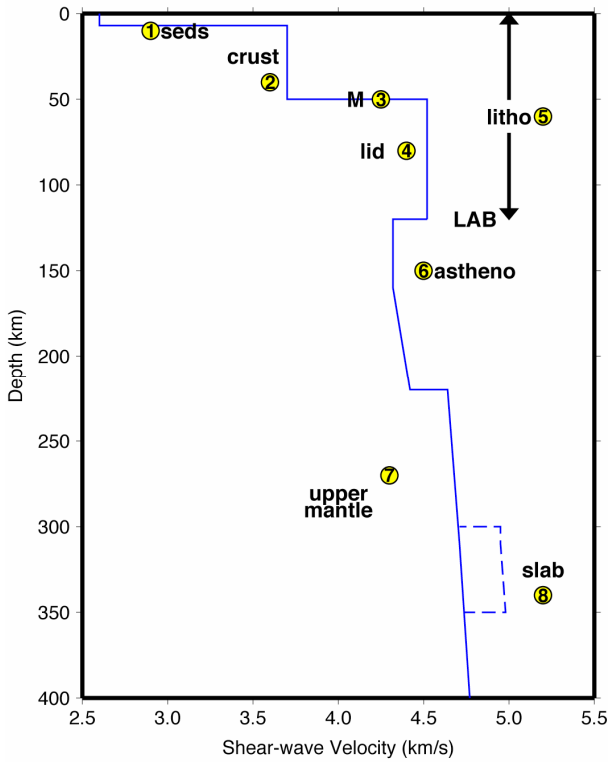

Fig. 4. An example of the velocity-depth profile for the grid search. Numbers correspond to items referred to in the text. M = Moho discontinuity. LAB = Lithospheric-Asthenospheric Boundary.

It is also important, as well, to state what we are not solving for. We are not solving for any detailed variations in velocity or Poisson's ratio in crust or lid. In other words, when we solve for the lid velocity, we are solving for Pn and Sn together since the Poisson's ratio in this layer is fixed to 0.26. Similarly, we do not allow any additional layers or velocity variations (say, in the crust) other than the ones discussed above.

The one item included as an additional constraint in the grid search are subducting slabs. The slab model used is the one included in the 3SMAC model (Nataf and Ricard, 1996), which specifies the location where slabs exist at various depths. Here, we incorporate the slabs by increasing the v_s by 5% (and v_p and density by 2%) at depths where the slabs exist (item 8 in **Fig. 4**).

We then proceed to perform this grid search every 1 degree in latitude and longitude over a region from latitude -20° to 85° and from longitude -20° to 150°, and assemble the results. Features of the crust and uppermost mantle in Eurasia and Africa, such as crustal

thickness and upper mantle velocities, have been discussed extensively in other papers (Pasyanos and Walter, 2002; Pasyanos and Nyblade, 2007). Here, we assemble the lithospheric thickness results and present them in the next section before comparing them to other estimates in the following sections.

3. Results

Results of the grid search for lithospheric thickness are shown in **Fig. 5**. Hot colors indicate thin lithosphere and cool colors indicate thick lithosphere. At first glance, the results look very reasonable. There is an obvious correspondence to the long-period group velocities as shown in **Fig. 3b**. Thick lithosphere is found in the West African Craton (which contains the overall thickest lithosphere in our model), Baltic Shield, Russian Platform, Congo Craton, Indian Shield, and Siberian Shield. Thin lithosphere is found along both divergent plate boundaries (oceanic rifts like the mid-Atlantic Ridge, the mid-Arctic, or Gakkel Ridge, and the Indian Ridge; continental rifts like the Red Sea and Baikal Rifts) and convergent plate boundaries (orogenic zones, subduction zones). We are even able to recover small-scale features like the Tarim Basin and Yangtze Craton.

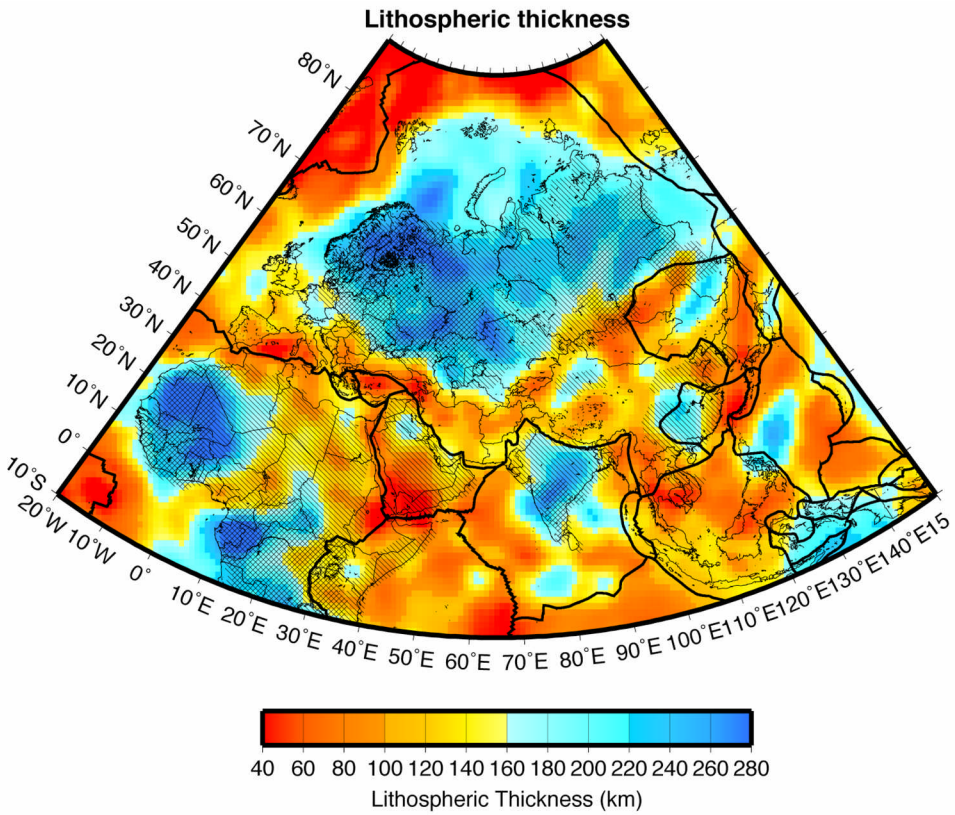

Fig. 5. Lithospheric thickness (in km) estimated from the modeling of long-period surface waves. Platform and shield areas are indicated by single and double hatched lines. Plate boundaries are indicated by the thick black lines.

We will highlight several other features here. In Europe, there is a sharp boundary in the lithospheric thickness along the Tornquist-Teisseyre Zone (TTZ), also referred to as the Trans European Suture Zone (TESZ), that separates the Precambrian East European Platform from Mesozoic-Cenozoic Western Europe. This has been confirmed with many other studies (e.g. Zielhuis and Nolet, 1994). This boundary continues southeast through the Black Sea into the Caucasus and west from there through the Caspian Sea and along the southern edge of the Kazakh Platform.

Within North Africa, we see a similar boundary between the East Saharan meta-craton, which refers to a craton that has been remobilized during an orogenic event (Abdelsalam et al., 2002), and the true cratons to the west (West African craton) and to the south (Congo craton). Clearly, the lithospheric thickness results indicate that the lithosphere was disrupted during this remobilization. Another craton that has experienced remobilization is the Sino-Korean Paraplatform, which consolidated in the Proterozoic, but remobilized in the Jurassic (Griffin et al., 1998). Like the East Saharan metacraton, we also find thin lithosphere in this region. The Arabian Shield and its African counterpart the Nubian Shield have also undergone lithospheric thinning by recent and current tectonism along the Red Sea and Gulf of Aden rift.

Off of the coast of northern Eurasia in the Arctic Ocean, the transition between continental thicknesses and oceanic thicknesses does not occur at the water's edge, but along the continental slope, as expected. Overall, there are interesting variations within Eurasia. We see, for example, some of the thickest lithosphere in the Baltic Shield, Russian Platform, and Ukrainian Shield. Moving more to the east, we don't see any significant thinning associated with the Paleozoic Urals. Within Siberia, we do see some variations with the Central Siberian Platform generally having a thicker lithosphere than the Western Siberian Platform. Farthest to the east, there is no significant thinning along the plate boundary between the Eurasian Plate and North American Plate in Siberia. This convergent plate boundary, which is considered to be region of broad deformation (Hindle et al., 2006), does not seem to have a large lithospheric signature.

In other regions recognized to have thin continental lithosphere, our model finds similarly thin lithospheric values. The best examples are for the Afar region, where studies like Dugda et al. (2007) confirm thinned lithosphere, the Eastern Anatolian High Plateau, where studies find little or no lithospheric lid (Sengor et al., 2003; Gok et al., 2007), and the Lake Baikal Rift (Lebedev et al., 2006).

4. Comparisons Among Methods

It appears that the surface-wave derived lithospheric thickness map has a strong correspondence to tectonic structure. To further assess the surface-wave derived lithospheric thicknesses, we compare our model to other estimates of lithospheric thickness. Here we consider four: a heat flow model, a lithospheric cooling model, a seismic tomography model, and estimates from S-wave receiver functions.

On continents, we compare the results to the thermal lithospheric model TC1 of Artemieva (2006). The lithospheric thickness from the TC1 model is plotted in **Fig. 6**, on the same scale as in **Fig. 5** for comparison. This model is based largely on the thermal modeling of borehole heat flow measurements (Pollack et al., 1993), which are very dense in Europe and Japan, and reasonably dense in Western Russia, China, India, and southeast Asia. Coverage is poor in most of North Africa and the Middle East. In areas without heat flow measurements, the model is based on geophysical analogy from the statistics of sampled regions of similar age and tectonics. Lithospheric thickness is then extracted from the thermal model using the 1300ºC isocontour. One consideration on the use of thermal models is whether the 1300ºC contour is the appropriate one to use. Using a lower temperature would obviously result in thinner lithospheric thickness estimates, whereas a higher temperature would result in thicker estimates.

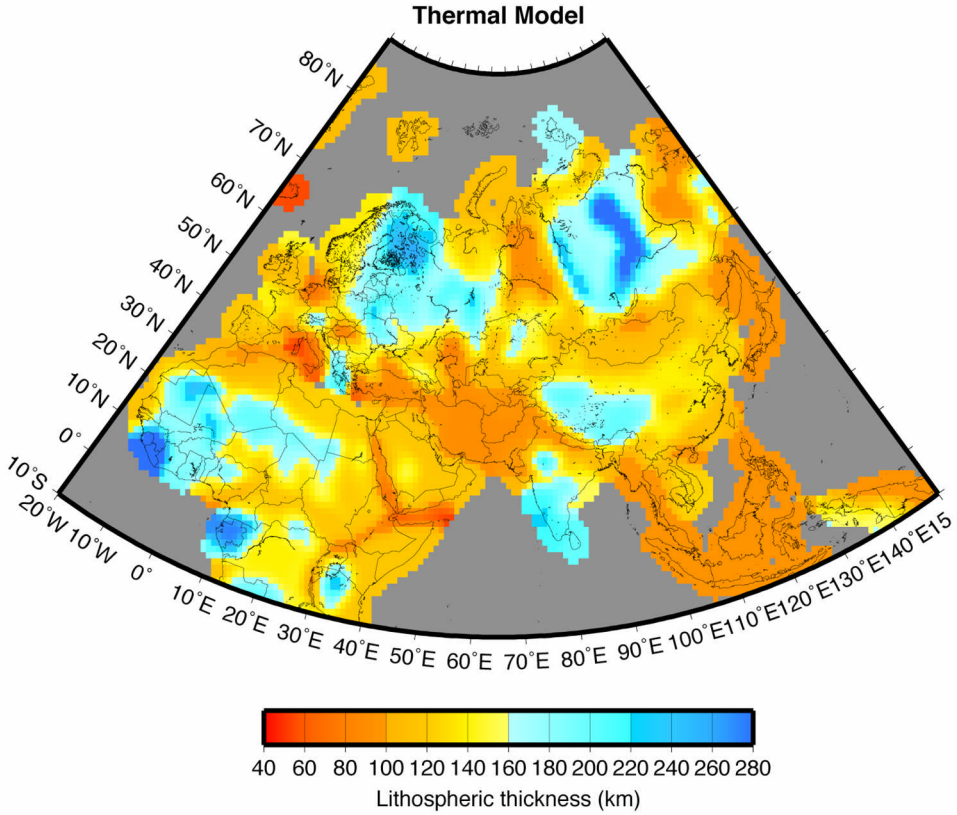

Fig. 6. Lithospheric thickness (in km) of the continents estimated from the thermal modeling of borehole heat flow measurements (TC1 model; Artemieva, 2006).

The visual comparison between the two models is good, although there are differences in the boundaries of anomalies and some absolute magnitude offsets. It also appears that the thermal lithospheric thickness variations are somewhat muted (higher lows and lower highs) when compared to the surface-wave derived model. Areas in which we find the largest differences are the West Siberian Platform and the Tibetan Plateau, and we shall examine these regions in more detail later on in the paper.

In oceans, we compare to a lithospheric cooling model that relates lithospheric age to lithospheric thickness. The lithospheric thickness z is estimated as:

$$z = 2.32\sqrt{\kappa t} \quad (1)$$

where the thermal diffusivity κ=1.0e-6 m^2s^{-1} (Turcotte and Schubert, 1982) and oceanic ages (t) come from Mueller et al. (1997). While deviations from this model have been documented for large ages, this formula provides a reasonable lithospheric thickness estimate for the large majority of oceanic region. Results of the lithospheric cooling model (plotted on the same scale) are shown in **Fig. 7**.

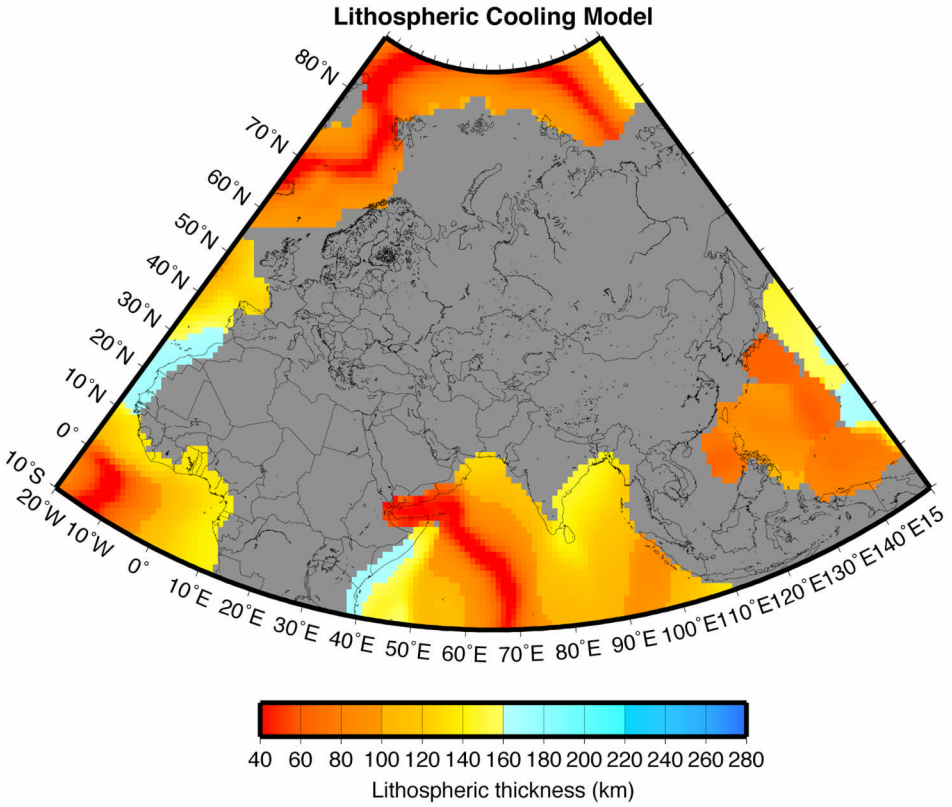

Fig. 7. Lithospheric thickness (in km) of oceanic crust derived from oceanic ages and a lithospheric cooling model.

The comparison is good in the Atlantic Ocean and Arctic Ocean, but only fair in the Indian Ocean and Pacific Ocean. For example, it appears that there are misfits (presumably errors in the seismic model here) in the Pacific Ocean near the Philippines and in parts of the Indian Ocean south of the Indian subcontinent.

We can also compare our lithospheric model to seismic tomography models. Here, we use the S20RTS model (Ritsema et al., 2004), but the results would be similar with other tomography models. We wanted a depth that would highlight lithospheric thickness differences, so we selected 150 km depth. The comparison here is very striking. While we couldn't compare lithospheric thickness directly, velocity perturbations from the

PREM model (Dziewonski and Anderson, 1981) match the lithospheric thickness maps very well. In many ways **Fig. 8** is a lower order (degree 20) version of the higher resolution surface wave derived model. The lateral resolution of a degree 20 model is nominally about 1000 km. Of course, the S20RTS model, like most other global tomography models, include long-period surface waves in the dataset, in this case Rayleigh wave phase velocities with $T \geq 40$ sec.

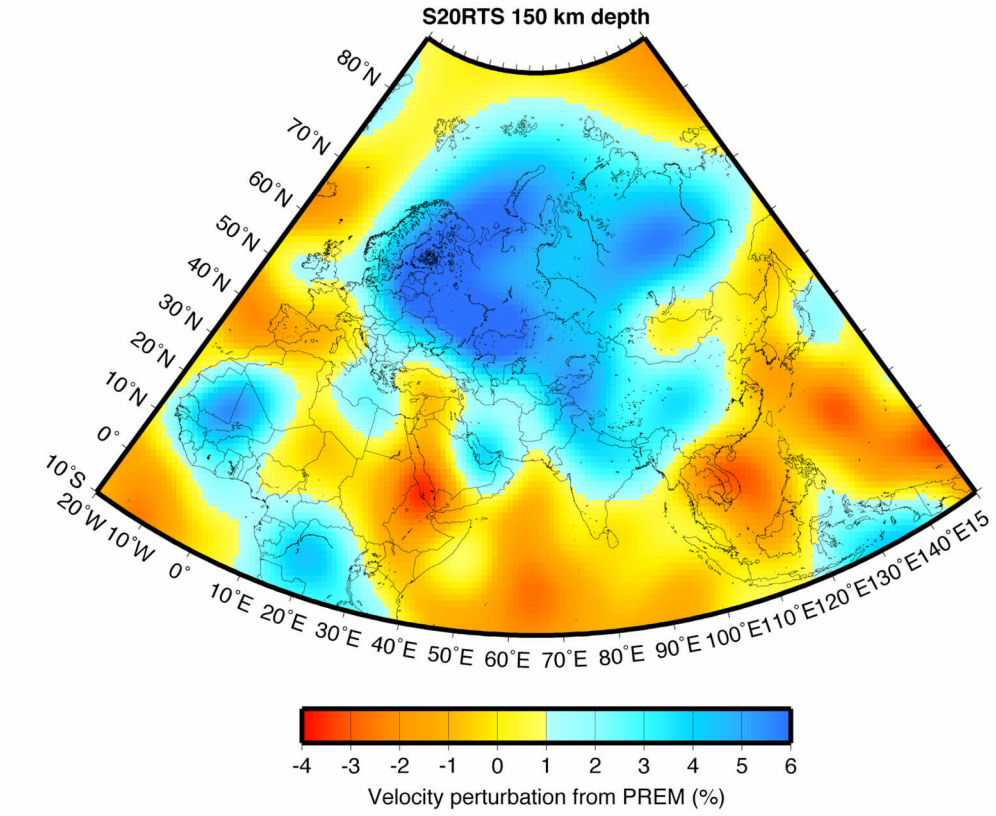

Fig. 8. Shear-wave velocity perturbations from the tomographic model S20RTS (Ritsema et al., 2004). Values are velocity differences (in %) from the PREM model.

Receiver functions are the response of the crust and upper mantle beneath a seismic station to an incident teleseismic phase. More commonly applied to incident P-waves, S-wave receiver functions (SRFs) have emerged as an analogous tool for incident S-waves (Farra and Vinnik, 2000). SRFs allow identification of lithospheric-asthenospheric boundary (LAB) because they arrive prior to direct (S) phase, and therefore do not interfere with multiple reflections as they do with P-wave receiver functions.

Here, we compare our lithospheric thickness estimates to two sets of SRF-derived lithospheric thickness estimates. The first is a study by Hansen et al. (2007) who calculated receiver functions for about 30 stations in Saudi Arabia. The second is a study by Kumar et al. (2007) who calculated SRFs for stations in and around the Indian Ocean basin.

Fig. 9 shows the individual station results from Hansen et al. (2007) plotted over the seismic and thermal maps of the Arabian Peninsula region. While the basic trends are present, neither of the other models fit the SRF-estimated thicknesses particularly well. The RMS of the seismic misfit (40 km) is lower than the RMS of the thermal misfit (50 km). In many ways, however, like the comparison to the global tomography models, it highlights resolution differences among the various estimates. If indeed the SRF estimates here are accurate, they vary laterally over such short distances that it would be difficult for any lower resolution model to fit the variations. At the very least, there is probably some doubt about lithospheric thickness variations of over 40 km between stations separated only 100 km or so apart.

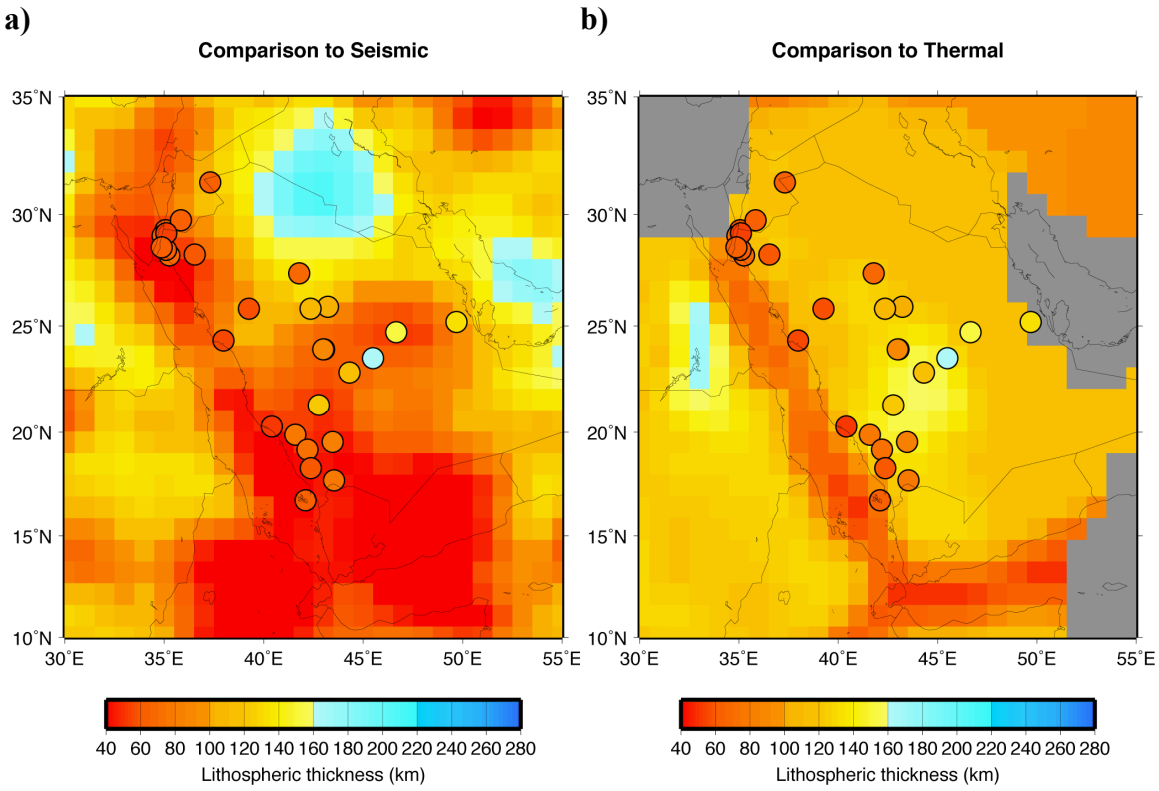

Fig. 9. Lithospheric thickness estimates made from S-wave receiver functions in Arabia (colored circles) compared to seismic (left) and thermal (right) estimates of the same region.

In the other study, Kumar et al. (2007) used SRFs to estimate lithospheric thickness at 35 stations and use them to infer lithospheric thickness around the Indian Ocean basin. Here, we seem to have the opposite issue. The lithospheric thicknesses inferred from the SRFs are assumed to represent this value so well and vary so little locally that values throughout the area can simply be interpolated between all the sparsely-spaced points. The lesson here is that resolution differences play a large role in the estimates between models.

Next, we make a direct point-to-point comparison of results where we plot the surface wave derived lithospheric thickness estimates vs. other estimates of this parameter. On

Fig. 10a, comparisons are made to the continental thermal model, the oceanic lithospheric cooling model, and the two S-wave receiver function studies. While **Fig. 10a** shows a lot of scatter in the data, much of the difference comes from resolution differences and offset boundaries. The overall RMS misfit is about 50 km.

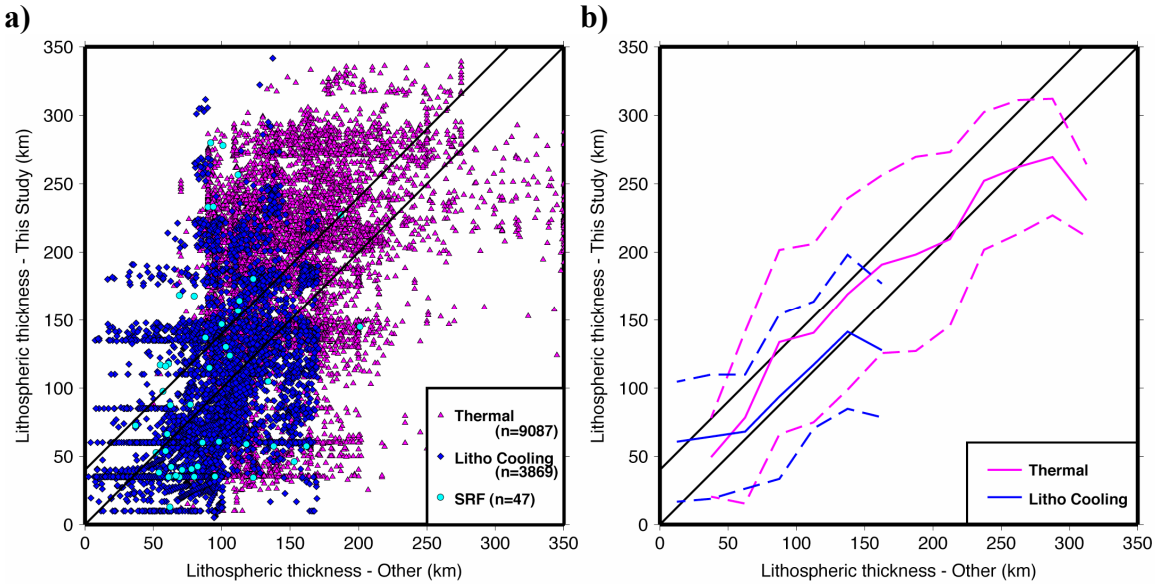

Fig. 10. a) A comparison of lithospheric estimates from this study to estimates from the TC1 thermal model (magenta triangles), the lithospheric cooling model (blue diamonds), and S-wave receiver functions (cyan circles). b) Mean and range of one standard deviation for thermal and lithospheric cooling thicknesses in 25 km bins. In both plots, the solid black lines indicate where the thicknesses are identical and where they are offset by 40 km.

Since there are so many points in **Fig. 10a**, we have also plotted the range of the thermal and lithospheric cooling values in **Fig. 10b**. The values have been calculated by determining the mean and standard deviation of the points in 25 km bins. The mean (solid lines) is plotted along with a range (dashed lines) from the mean plus and minus one standard deviation. There were too few points for the S-wave receiver functions to make a useful calculation in this regard. Also plotted on the figures (as black lines) are the lines for a perfect correspondence and one in which the seismic thickness is 40 km greater than the thermal thickness. This is the value estimated by Jaupart et al. (1998) as the average depth thickness between the conductive thermal boundary layer and the top of the convective mantle. While the lithospheric cooling values track closer to the center line, the average of the thermal model for the continents is closer to the offset one. Solid evidence for any offset between the two is weak, however, because the scattering is probably too high to make this meaningful.

In addition to the scatter, however, is a notable "rolling over" in the trend where, when comparison thicknesses continue to climb, the surface wave estimates flatten. There also seems to be a better overall fit for thinner lithosphere. When we look at the rms misfit as a function of lithospheric thickness, the misfit is relatively flat for all thicknesses of the lithospheric cooling model. We find, however, the misfit of the thermal model increases

from about 50 km to about 100 km for thicknesses greater than 300 km. Referring back to **Fig. 1b**, there is excellent discrimination power between lid thickness at 100 sec, when the values are less than 200 km, but much poorer when the thicknesses are larger. It seems like longer periods may be needed to differentiate among lithospheric thicknesses greater than around 200 km.

5. Regional Comparisons

Now that we have compared methodologies in general, we would like to take a detailed look at several regions. Here we examine the Congo Craton in Central Africa, the Western Siberian Platform in northern Eurasia, and the Tibetan Plateau in Central Asia.

The Congo Craton is a region that seems to vary somewhat among the various estimates. Like most cratons, the Congo Craton has a thick lithospheric keel. In our lithospheric model, however, the keel is not one continuous structure, but rather thins from the East African rift to an area under the Cuvette Centrale (Central Basin) of the Congo Craton (**Fig. 11a**). This is discussed in some detail in Pasyanos and Nyblade (2007). We find some corroborating evidence for this in the thermal models (**Fig. 11b**). The seismic tomography model S20RTS has a more-or-less continuous high-velocity for this area, but wouldn't necessarily have the resolution to see such a small-scale feature.

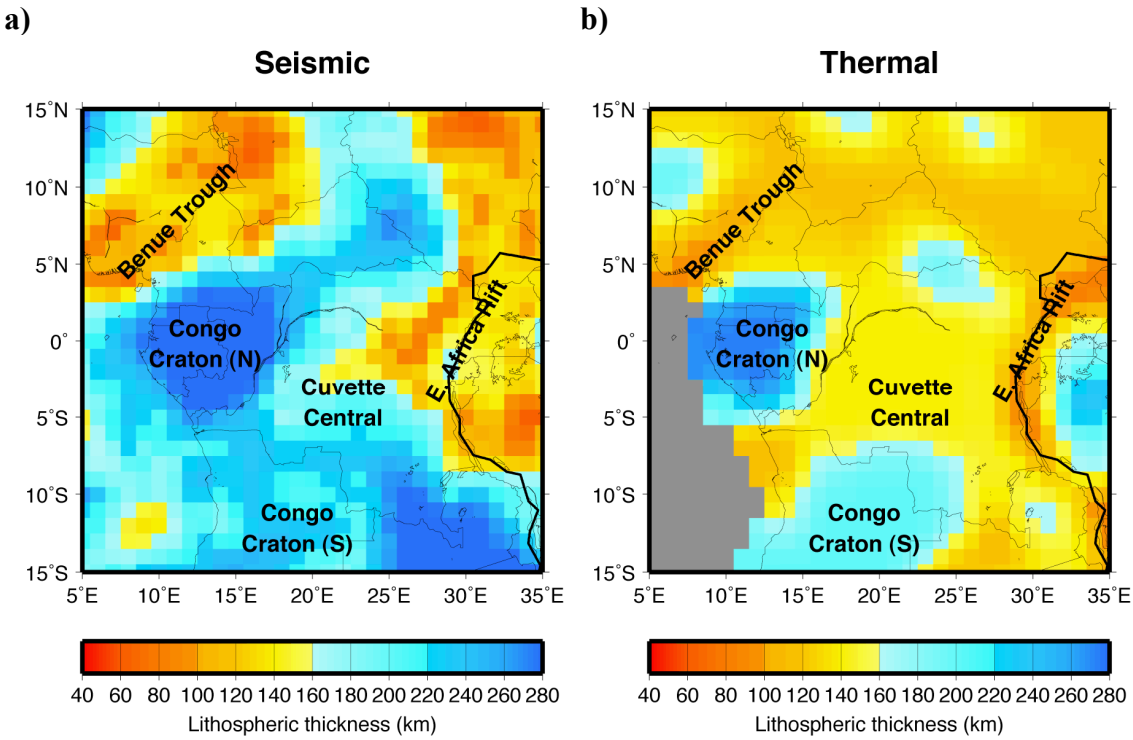

Fig. 11. A comparison of lithospheric thickness estimates for Central Africa from a) this study and b) the TC1 heat flow model.

Results from other seismic models are mixed. A study by Priestley et al. (2008) using waveform modeling of fundamental and higher-model surface waves finds a continuous

region of thick lithosphere in central and southern Africa, but other inversions of the same data find slow velocities under the Cuvette Centrale (Stewart Fishwick, personal communication). Perhaps the resolution to the inconsistency lies in model resolution or in the differing depth sensitivity. This area has been partially remobilized (Daly et al., 1992) and the multi-modal surface waves, which are sensitive to deeper structure, still require a high-velocity lithospheric keel at depth, while this study, primarily sensitive to shallower mantle structure, sees the more shallow affected mantle. It is likely that the thermal structure is also sensitive to the more recent activity.

As an experiment, we reran the structural inversions for Central Africa using surface wave dispersion that extends out to 150 sec. Group velocities at this period have a maximum sensitivity of about 150 km – deeper than the 120 km maximum sensitivity of 120 sec. waves (**Fig. 1a**). The results are not substantially different that those plotted in **Fig. 11a**, although the area of the Congo Craton that has thinned lithosphere narrows to a small region near the eastern portion of the Congo River.

The next subregion that we investigate is West-Central Siberia. Here, all models find thick lithosphere in the Siberian Shield, slightly thinner in the Taymyr Fold Belt, and very thin along the Baikal Rift. This is all consistent with other tectonic studies of this region (e.g. Lebedev et al., 2006). Where results differ significantly is in the West Siberian Platform. Fast long-period surface wave velocities indicate thicker lithosphere (**Fig. 12a**), while moderately high (50 – 60 mW/m^2) surface heat flow (Artemieva and Mooney, 2001) indicates thinner lithospheric thickness than typical shield and platform structures (**Fig. 12b**). At 150 km depth, the S20RTS model has a continuous region of high-velocities running from the Baltic Shield to Eastern Siberia but, again, there is the question of whether this model has the resolution to see such features. Unlike the Cuvette Central, the West Siberian Platform is a relatively large-scale feature that is at least as big as some features seen in **Fig. 8**. It is still open, however, whether there is coverage of this (relatively aseismic) region in particular.

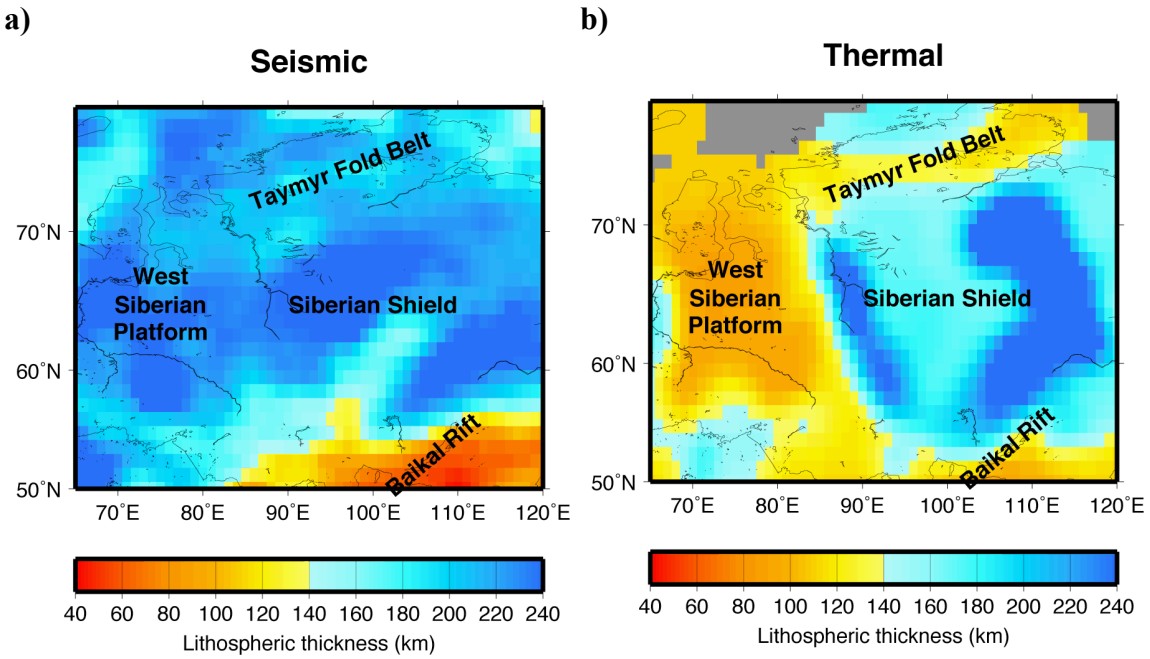

Fig. 12. A comparison of lithospheric thickness estimates for West-Central Siberia from a) this study and b) the TC1 heat flow model.

One possible explanation for the discrepancy is significant heat production in the crust, which would create high surface heat flow without requiring a thin lithosphere. Another possibility is that the borehole measurements in this region are not in thermal equilibrium (Irina Artemieva, personal communication) and, therefore, are not representative of the regional heat flow. It is also possible that in some regions the thermal modeling, which usually assumes a linear heat flow / heat production relationship, does not adequately explain the relationship between heat production at depth and surface heat flow.

The last region we compare in detail is the Tibetan Plateau and surrounding areas in Central Asia. The surface wave study finds a marked thinning of the lithosphere under the plateau compared to India to the south, and the Tarim and Sichuan Basins to the north and east (**Fig. 13a**). This is consistent with many recent seismic and gravity models that show a thickening of the lithosphere under the Himalayas and southwest Tibet and then abruptly thinning under the Tibetan Plateau (e.g. An and Shi, 2006; Zhang et al., 2007; Jiménez-Munt et al., 2008). This supports the model of the thrusting and detachment of the Indian mantle lithosphere under Eurasia (Owens and Zandt, 1997).

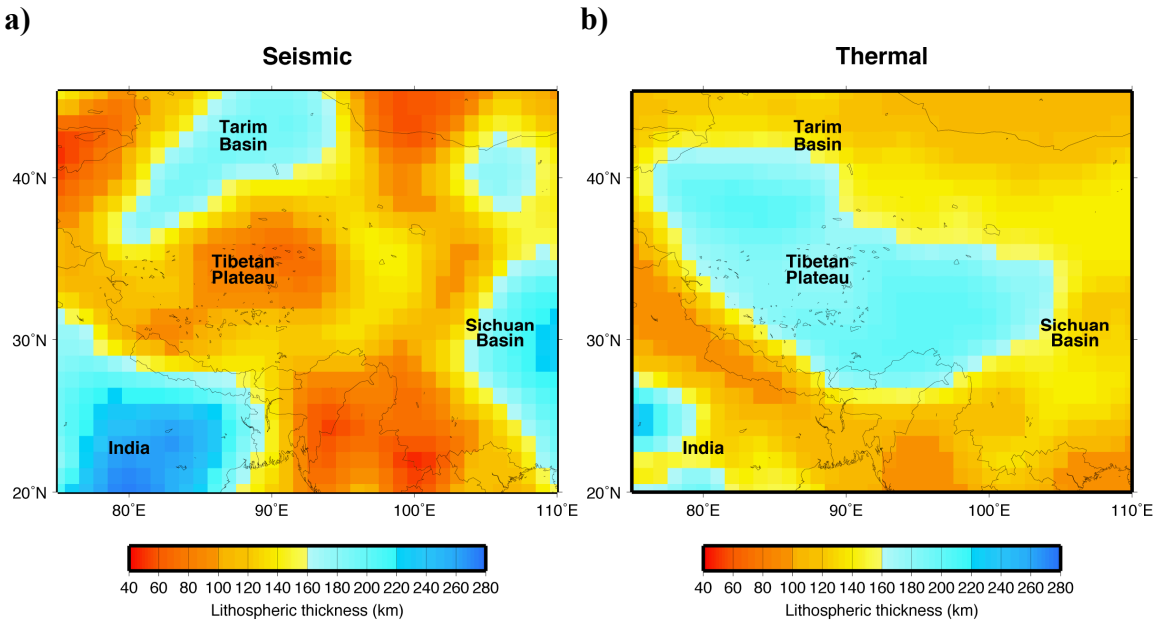

Fig. 13. A comparison of lithospheric thickness estimates for the Tibetan Plateau from a) this study and b) the TC1 heat flow model.

The lithospheric thicknesses from the thermal model are very different for this region, showing an increase in lithospheric thickness under the plateau (**Fig. 13b**). The high (~ 80 mW/m^2) surface heat flow (Artemieva and Mooney, 2001) for this region is somewhat higher than surrounding regions, which usually indicates a thinning of the lithosphere. In many respects, however, Tibet as a region is the exception that might prove the rule. Due to the detachment of the Indian lithosphere, this might not be a region well-modeled by simple thermal (or seismic) modeling assumptions. Also, perhaps because of its very dramatic recent tectonic history, this is one region where the thermal lithosphere is indeed different than the lithosphere calculated from seismic or gravity methods.

6. Discussion

Long period surface wave data can be used to provide estimates on lithospheric thickness, particularly where other estimates might not be available or reliable. Even using simple models to invert the dispersion models for lithospheric structure, we are able to recover major tectonic features. Most notably, we easily recover the deep lithospheric keels under cratons and the thinned lithosphere along plate boundaries. We also find several Precambrian regions (East Saharan Metacraton and Sino-Korean Paraplatform) where the lithospheric lid was disrupted by more recent remobilization.

We also compared our results to several other estimates of lithospheric thickness, both seismic and otherwise. Qualitatively, the maps between seismic estimates and other estimates (like thermal) are similar. Quantitatively, there are still some existing differences among the various estimates. There are a number of possible explanations for the observed differences. First, given the simple procedure employed, there are probably aspects to modeling the seismic lithosphere that are not being captured using the current methods. As mentioned earlier, surface waves are not sensitive enough to invert for

detailed crust and upper mantle structure, and large variations in our assumptions (v_p/v_s ratio, lid structure) could bias our lithospheric estimates. Ideally, one would like to model the structure with multiple datasets which can select among models which are non-unique using individual datasets. Unfortunately, this can probably only be done in selected regions, and not yet easily applied to broad regions. Also, it seems clear that the group velocities used in the inversion should extend to longer periods. We did not employ them here because the maps at longer periods are not as reliable as those in the range that was used.

Of course, another explanation is that there are errors in the thermal thickness maps and estimates from SRFs that we are comparing our results to. For example, how might using an isocontour other than 1300° C for the lithospheric boundary affect our comparison? It is also clear that in some of our comparisons, there are some consistencies in results derived from like-data (e.g. seismic), but hard to reconcile with other estimates. This brings up the suggestion that, in some cases at least, the seismic and thermal lithosphere may be fundamentally different quantities. Lastly, the comparisons highlighted the fact that there are issues comparing the estimates because of radically-differing model resolutions. It is likely that the differences we find are due to a combination of these factors.

In future work, we would like to incorporate longer-period data (T > 120 - 150 sec) which will likely improve estimates in regions with large lithospheric thickness. This will occur when the long period group velocity maps improve. In addition, it would be worth exploring some changes to the parameterization to reduce some of the systematic misfit between seismic and other estimates. This could consist of introducing more complexity in the modeling, such as including transverse isotropy in the mantle, more crustal layers, and/or variable Poisson's ratio in the crust and upper mantle. Lastly, it would be worth exploring in finer details some of areas discussed in the Regional Comparisons section that has some discrepancies or inconsistencies among the various methods. In these areas, it would be worth bringing many data sets to bear on the problem to find the models most consistent with the ensemble of data.

Acknowledgements

We gratefully acknowledge discussions with Irina Artemieva and Stewart Fishwick. This work performed under the auspices of the U.S. Department of Energy by Lawrence Livermore National Laboratory under Contract DE-AC52-07NA27344, LLNL-JRNL-*******.

References

Abdelsalam, M.G., Liégeois, J.-P., Stern, R.J., 2002. The Saharan metacraton, J. Afr. Earth Sci, 34, 119-136.

An, J., Shi, Y., 2006. Lithospheric thickness of the Chinese continent, Phys. Earth. Planet. Int., 159, 257-266, doi:10.1016/j.pepi.2006.08.002.

Artemieva, I.M., Mooney, W.D., 2001. Thermal thickness and evolution of Precambrian lithosphere: A global study, J. Geophys. Res., 106, 16,387-16,414.

Artemieva, I.M., 2006. Global 1° x 1° thermal model TC1 for the continental lithosphere: Implications for lithosphere secular evolution, Tectonophys., 245-277, doi:10.1016/j.tecto.2005.11.022.

Conrad, C.P., Lithgow-Bertelloni, C., 2006. Influence of continental roots and asthenosphere on plate-mantle coupling, Geophys. Res. Lett., 33, L05312, doi:10.1029/2005GL02561.

Daly, M., Lawrence, S., Diemu-Tshiband, K., Matouana, B., 1992. Tectonic evolution of the Cuvette Centrale, Zaire, J. Geol. Soc. Lond., 149, 539-546.

Dugda, M.T., Nyblade, A.A., Julia, J., 2007, Thin lithosphere beneath the Ethiopian plateau revealed by a joint inversion of Rayleigh wave group velocities and receiver functions, J. Geophys. Res., 112, B08305, doi:10.1029/2006JB004918.

Dziewonski, A.M., Anderson, D.L., 1981. Preliminary reference earth model, Phys. Earth Planet. Int, 25(4), 297-356.

Farra, V., Vinnik, L., 2000. Upper mantle stratification by P and S receiver functions, Geophys. J. Int., 141, 699-712.

Gok, R., Pasyanos, M.E., Zor, E., 2007. Lithospheric structure of the continent-continent collision zone: Eastern Turkey, Geophys. J. Int., doi:10.1111/j.1365-246X.2006.03288.x.

Griffin, W.L., Andi, Z., O'Reilly, S.Y., Ryan, C.G., 1998. Phanerozoic evolution of the lithosphere beneath the Sino-Korean Craton, in Mantle Dynamics and Plate Interactions in East Asia (Flower, M., Chung, S.L., Lo, C.H., and Lee, T.Y. eds.) in American Geophysical Union Geodynamics Series, Vol. 27, 419 pp.

Hansen, S.E., Rodgers, A.J., Schwartz, S.Y., Al-Amri, A., 2007. Imaging ruptured lithosphere beneath the Red Sea and Arabian Peninsula, Earth. Planet. Sci. Lett., 259, 256-265, doi:10.1016/j.epsl.2007.04.035.

Hindle, D., Fujita, K., Mackey, K., 2006. Current deformation rates and extrusion of the northwestern Okhotsk plate, northeast Russia, Geophys. Res. Lett., 33, L02306, doi:10.1029/2005GL024814.

Jaupart, C., Mareschal, J.-C., 1999. The thermal structure and thickness of continental roots, Lithos 48 (1-4), 93-114.

Jaupart, C., Mareschal, J.-C., Guillou-Frottier, L., Davaille, A., 1998. Heat flow and thickness of the lithosphere in the Canadian Shield, J. Geophys. Res., 103, 15,269-15,286.

Jiménez-Munt, I., Fernàndez, M., Vergés, J., Platt, J.P., 2008. Lithosphere structure underneath the Tibetan Plateau inferred from elevation, gravity and geoid anomalies, Earth. Planet. Sci. Lett., 267, 276-289.

Kennett, B.L.N., Engdahl, E.R., Buland, R., 1995. Travel times for global earthquake location and phase association, Geophys. J. Int., 122, 108-124.

Kumar, P., Yuan, X., Kumar, M.R., Kind, R., Li, X., Chadha, R.K., 2007. The rapid drift of the Indian tectonic plate, Nature, 449, doi:10.1038/nature06214.

Laske, G., Masters, G., 1997. A global digital map of sediment thickness, EOS Trans. AGU, 78, F483.

Lebedev, S., Meier, T., van der Hilst, R.D., 2006. Asthenospheric flow and origin of volcanism in the Baikal Rift area, Earth Planet. Sci. Lett., 249 (3-4): 415-424, doi:10.1016/j.epsl.2006.07.007.

Mueller, R.D., Roest, W.R., Royer, J.-Y., Gahagan, L.M., Sclater, J.G., 1997. Digital isochrons of the world's ocean floor, J. Geophys. Res., 102, 3211–3214.

Nataf, H.-C., Ricard, Y., 1996. 3SMAC: an a priori tomographic model of the upper mantle based on geophysical modeling, Phys. Earth Planet. Inter., 95, 101-122.

Owens, T.J., Zandt, G., 1997. The implications of crustal property variations on models of Tibetan Plateau evolution, Nature, 387, 37-43.

Pasyanos, M.E., 2005. A variable-resolution surface wave dispersion study of Eurasia, North Africa and surrounding regions, J. Geophys. Res., 110, B12301, doi:10.1029/2005JB003749.

Pasyanos, M.E., Walter, W.R., 2002. Crust and upper-mantle structure of North Africa, Europe, and the Middle East from inversion of surface waves, Geophys. J. Int., 149, 462-480.

Pasyanos, M.E., Nyblade, A.A., 2007. A top to bottom lithospheric study of Africa and Arabia, Tectonophysics, 444, 27-44, doi:10.1016/j.tecto.2007.07.008.

Pollack, H.N., Hurter, S.J., Johnson, J.R., 1993. Heat flow from the earth's interior: analysis of the global data set, Rev. Geophys., 31, 267-280.

Priestley, K., McKenzie, D., Debayle, E., Pilidou, S., 2008. The African upper mantle and its relationship to tectonics and surface geology, submitted to Geophys. J. Int.

Ritsema, J., van Heijst, J.J., Woodhouse, J.H., 1999. Complex shear wave velocity structure imaged beneath Africa and Iceland, Science, 286, 1925-1928.

Şengör, A.M.C., Ozeren, S., Genc, T., Zor, E., 2003. East Anatolian high plateau as a mantle-supported, north-south shortened domal structure, Geophys. Res. Lett., 30(24), 8045, doi:10.1029/2003GL017858.

Turcotte, D.L., Schubert, G., 1982. Geodynamics: Applications of Continuum Physics to Geological Problems, 450 pp., John Wiley & Sons, New York.

Weeraratne, D.S., Forsyth, D.W., Fischer, K.M., Nyblade, A.A., 2003. Evidence for an upper mantle plume beneath the Tanzanian craton from Rayleigh wave tomography, J. Geophys. Res., 108(9), 2427, doi:10.1029/2002JB002273.

Zhang, X.M., Sun, R.M., Teng J.W., 2006. Study on crustal, lithospheric and asthenospheric thickness beneath the Qinghai-Tibet Plateau and its adjacent areas, Chin. Sci. Bull., 52 (6), 797-804 , doi: 10.1007/s11434-007-0110-7.

Zielhuis, A., Nolet, G., 1994. Deep seismic expression of an ancient plate boundary in Europe, Science, 265 (5168), 79-81, DOI:10.1126/science.265.5168.79.

Figure captions

Fig. 1. a) Velocity profile and associated sensitivity kernels for long period Rayleigh waves; b) Dispersion for a model where the thickness of the lid is varied from 0 – 300 km.

Fig. 2. a) Rayleigh wave (triangles) and Love wave (circles) measurements and model fits (solid and dashed lines, respectively) of dispersion (left) and S-wave velocity profile (right) from Eastern Europe. b) Same plots for Western Europe.

Fig. 3. a) Map of surface wave dispersion paths (blue lines) for 80 sec Rayleigh waves with events (yellow circles) and stations (red triangles) indicated. b) Map of surface wave group velocity (in km/s) for 80 sec Rayleigh waves.

Fig. 4. An example of the velocity-depth profile for the grid search. Numbers correspond to items referred to in the text. M = Moho discontinuity. LAB = Lithospheric-Asthenospheric Boundary.

Fig. 5. Lithospheric thickness (in km) estimated from the modeling of long-period surface waves. Platform and shield areas are indicated by single and double hatched lines. Plate boundaries are indicated by the thick black lines.

Fig. 6. Lithospheric thickness (in km) of the continents estimated from the thermal modeling of borehole heat flow measurements (TC1 model; Artemieva, 2006).

Fig. 7. Lithospheric thickness (in km) of oceanic crust derived from oceanic ages and a lithospheric cooling model.

Fig. 8. Shear-wave velocity perturbations from the tomographic model S20RTS (Ritsema et al., 2004). Values are velocity differences (in %) from the PREM model.

Fig. 9. Lithospheric thickness estimates made from S-wave receiver functions in Arabia (colored circles) compared to seismic (left) and thermal (right) estimates of the same region.

Fig. 10. a) A comparison of lithospheric estimates from this study to estimates from the TC1 thermal model (magenta triangles), the lithospheric cooling model (blue diamonds), and S-wave receiver functions (cyan circles). b) Mean and range of one standard deviation for thermal and lithospheric cooling thicknesses in 25 km bins. In both plots, the solid black lines indicate where the thicknesses are identical and where they are offset by 40 km.

Fig. 11. A comparison of lithospheric thickness estimates for Central Africa from a) this study and b) the TC1 heat flow model.

Fig. 12. A comparison of lithospheric thickness estimates for West-Central Siberia from a) this study and b) the TC1 heat flow model.

Fig. 13. A comparison of lithospheric thickness estimates for the Tibetan Plateau from a) this study and b) the TC1 heat flow model.